ARTICLE

Preparation and Characterization of *Stellera Chamaejasme*-Based Carbon Molecular Sieves

Baian Shen, Haichao Li[*], Zixiang Guo, Jingxiao Li and Yuting Bao

Key Laboratory of Applied Physical Chemistry of Qinghai Provincial, Qinghai Nationalities University, Xining, 810007, China

[*]Corresponding Author: Haichao Li. Email: lihaichao@vip.163.com

ABSTRACT

The activation effect of boric acid as an activator is good, and we investigate the best activation conditions for the boric acid impregnation method. To represent the structural characteristics and adsorption performance of the *Stellera Chamaejasme* based carbon molecular sieves, we use Brunner-Emmet-Teller (BET) measurements, scanning electron microscope (SEM), Raman spectra (Raman), X-ray diffraction (XRD), and adsorption property measurement. When the loading ratio was 0.68:1, the specific surface area was 532.21 m^2/g, the total pore volume was 0.24 cm^3/g, the average pore size was 1.81 nm, the adsorption value of methylene blue was 145.28 mg/g, and the adsorption value of iodine was 713.33 mg/g, the results showed that boric acid had better activation effect. The carbon molecular sieves made from *Stellera Chamaejasme* and activated with boric acid produce two peaks on the aperture distribution graph that are densely distributed in the micropore range. This indicates that boric acid's pore-forming tendency is primarily micropore.

KEYWORDS

Carbon molecular sieve; *Stellera Chamaejasme*; boric acid; impregnation method

1 Introduction

A new type of carbon adsorbent is the carbon molecular sieve. It is a microporous activated carbon with well-developed pores and distinct surface properties [1] Because of its light weight, excellent adsorption performance, good catalytic property, and outstanding electrochemical capacity, it is widely used in chemistry, chemical industry, agriculture, industry, and other fields, such as the SAPO-34 molecular sieve prepared by Xing et al. [2], the gas conditioner by Zhou et al. [3], and the carbon molecular sieve applied to chromatographic analysis by Song et al. [4]. Impregnation method, melting method, supramolecular self-assembly method, and mesoporous agent method, discovered by Liu et al. [5], are now the most widely used carbon molecular sieve preparation methods, with impregnation method and melting method being the most widely used. Many studies on the preparation of carbon molecular sieves with $ZnCl_2$, H_3PO_4, and other activators were conducted. Only Ma et al. [6–11] have looked into the preparation of carbon molecular sieves using H_3BO_3 as an activator, so there is a significant gap in this area. However, boric acid and borate, as an excellent flame retardant, can effectively change the structure and sequence of carbon in biological materials, generate stable carbon, and prevent its oxidation reaction from releasing CO, CO_2, and other gases into the atmosphere, resulting in a low carbon formation rate.

The Tibetan Plateau, dubbed the "Third Pole of the World," is China's largest grassland animal husbandry production base and a key ecological barrier [12]. Due to global climate change, human destruction, and other factors, 50.4% of grassland has been degraded in recent years, with 16.5% of grassland severely degraded. As a result, the alpine grassland's ecological environment is deteriorating on a daily basis, with large-scale erosion and the spread of toxic plants in some areas, as well as the degradation of high-quality natural grassland to poisonous weed grassland, posing a slew of problems for livestock production and ecological environment construction and protection [13]. *Stellera Chamaejasme* is the representative plant of the typical alpine steppe degradation stage. *Stellera Chamaejasme*, also known as steamed bread, graceful jessamine herb, and other names, is a perennial herbaceous plant. Salivation, vomiting, and shortness of breath are the most common symptoms of animal poisoning, and pregnant animals may experience abortion or even death due to exhaustion in severe cases [14]. Meanwhile, livestock has turned green *Stellera Chamaejasme* seedlings poisoned, more for acute poisoning, main symptoms of vomiting, abdominal pain, diarrhea, limb weakness, can't afford to lie down, whole body spasm, head bent back, heart palpitations hyperthyroidism with blood, feces, serious when collapse or convulsion death, female can cause abortion when in touch with humans, root powder and pollen produce allergic dermatitis and cause a strong and long-lasting unpleasant irritation in the eyes, nose, and throat [15]. Today, *Stellera Chamaejasme* has gradually evolved into the dominant plant in severely degraded grassland [16]. For example, in Gansu province and Qinghai Province in China, 466,000 hectares of grassland were damaged, 137.5 million kg of forage production were lost, and the economic loss was 15 million to 20 million yuan [17]. *Stellera Chamaejasme* grows on natural grassland in Qinghai province and has a density of 3.5 clusters per m^2, with a maximum density of 50 clusters per m^2. Currently, the only way to prevent and control *Stellera Chamaejasme* is to remove it, but the *Stellera Chamaejasme* that is removed cannot be turned into valuable resources. Although *Stellera Chamaejasme* has potential in terms of medicinal value [18], industrial value, and ecological resource value, its deep utilization is still being explored, so finding a resource utilization method for *Stellera Chamaejasme* is critical. According to Li et al. [19,20], the root of *Stellera Chamaejasme* contains a large amount of cellulose, lignin, polysaccharide, and other chemical components, making it ideal for the preparation of porous carbon materials [21], allowing *Stellera Chamaejasme* to achieve high value and resource utilization. As a result, this study made a new attempt to prepare carbon molecular sieve with boric acid as the activator, providing a new idea for future research by relevant scholars.

2 Experimental

All chemicals were of analytical grade and used as received.

2.1 Preparation of Stellera Chamaejasme-Based Carbon Molecular Sieves

Boric acid aqueous solutions with concentrations of 10%, 20%, 30%, and 40% were prepared, respectively. In a Chinese medicine grinder, two groups of *Stellera Chamaejasme* roots weighing 10 g were ground into fine powder and screened through a 0.2 mm sieve. The goal is to increase the surface area of contact between *Stellera Chamaejasme* and aqueous boric acid solution. The powdered *Stellera Chamaejasme* was immersed in a boric acid aqueous solution and impregnated for 12 h at room temperature. The boric acid aqueous solution was extracted by vacuum filter after 12 h, and the impregnated *Stellera Chamaejasme* powder was filtered out and dried for 1 h at 80°C in a constant temperature drying oven.

The sample was given the designation LB-X, with X denoting the amount of boric acid loaded onto the carbon.

To obtain semi-finished carbon molecular sieve, the samples LB-0.5, LB-0.55, LB-0.68, and LB-0.7 were placed in a muffle furnace and heated from room temperature to 500°C in 100 min, activated at this temperature for one hour, and then cooled to room temperature naturally. The sample was immersed in

500 mL ultrapure water and heated in a thermostatic electric heating jacket for 1 h at a constant temperature of 100°C. If the pH value of the wash carbon water is not neutral, use a vacuum filter filter to filter the sample out, and then repeat the carbon washing step until the pH value of the wash carbon water is neutral. After filtering the samples, they were placed in a thermostatic drying oven and dried for 1 h at 80°C. They were then ground until the sample size was 71 μm, and the *Stellera Chamaejasme*-based carbon molecular sieve was prepared using the impregnation method.

2.2 Adsorption Experiments

To investigate the adsorption kinetics of the prepared carbon molecular sieve, an UV-visible spectrophotometer was used to create a standard curve of methylene blue, and the relationship between adsorption time and adsorption capacity was investigated.

To ensure saturation adsorption, 1 g carbon molecular sieve was placed in a conical flask containing 100 ml methylene blue solution, placed in a thermostatic oscillator, and kept oscillating at 25°C for 24 h. At 665 nm, the absorbance of a 2 mL adsorbed solution was measured, and the adsorbed concentration was calculated using the standard curve.

The iodine adsorption experiment followed the same steps.

2.3 Adsorption Kinetics Experiment

1 g carbon molecular sieve was placed in a conical flask containing 100 mL methylene blue solution, placed in a thermostatic oscillator, and kept oscillating at 25°C. In a quartz cuvette, 2 mL of solution was filtered at 5 min intervals. The UV-visible spectrophotometer was used to calculate the concentration, and then a standard curve was used to calculate the adsorption capacity.

3 Results and Discussion

Carbon molecular sieves based on *Stellera Chamaejasme* were made by impregnating them with boric acid. The results show that the method produced carbon molecular sieve with an ultra-porous structure successfully. By optimizing impregnation parameters, carbon molecular sieve has a higher adsorption efficiency under the condition of constant activation temperature. The methylene blue adsorption test is one of the most common methods for determining the properties of wood activated carbon, and its adsorption value is a useful metric for describing the properties of wood carbon materials. Because methylene blue molecules have an average diameter of 0.928 nm, the adsorption value of methylene blue can be used to characterize the degree of development of micropores smaller than 2 nm in the prepared materials. The adsorption value of methylene blue gradually increases with the increase in impregnation amount (Fig. 1a), but there is still a large gap between the adsorption value of methylene blue and that of samples prepared by other scholars [22]. This could be due to the fact that the *Stellera Chamaejasme*-based carbon molecular sieve has two pore size distribution peaks. The peak with an average pore size of about 1 nm is critical for methylene blue adsorption, whereas the peak with an average pore size of about 0.6 nm has a methylene blue molecule that is too large to have a significant adsorption effect.

The iodine adsorption value was measured by iodometry in order to investigate the adsorption effect of ultrafine pores less than 1 nm in this paper. Because iodine molecules are about 0.6 nm in size, they have a good characterization effect on micropores smaller than 1 nm. It can be seen from the iodine adsorption value determination (Fig. 1b) that as the impregnation amount increases, so does the iodine adsorption value. The iodine adsorption value of *Stellera Chamaejasme*-based carbon molecular sieve has a good performance when compared to other scholars [23], indicating that the two pore size distribution peaks with average pore sizes of 0.6 and 1.0 nm respectively play an adsorption role in the iodine adsorption process.
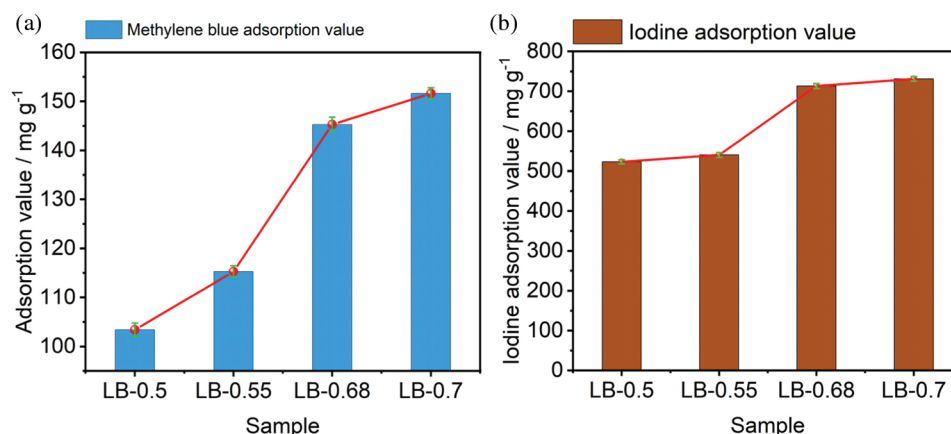
Figure 1: (a) Methylene blue adsorption values; (b) Iodine adsorption value

The specific surface area of a carbon molecular sieve influences its adsorption capacity and is one of the most important indicators of its adsorption performance. The specific surface area of carbon molecular sieves is described using terms such as microporous specific surface area, mesoporous specific surface area, macro-porous specific surface area, and macro-porous specific surface area. According to the findings, a carbon molecular sieve's specific surface area, which is usually determined by its porosity, is one of the most important factors influencing its adsorption performance.

BET analysis can be used to determine the total pore volume, specific surface area, average pore size, and other parameters of the carbon molecular sieve. Table 1 shows that as the loading capacity increases, the pore volume parameters increase, indicating that the use of boric acid as an activator is significant and effective.

**Table 1:** Pore volume parameters reflected in BET

Sample	Specific surface area (m^2/g)	Total entrance (cm^3/g)	Average pore size nm	Monolayer adsorption capacity (cm^3(STP)/g)
LB-0.5	455.86	0.2083	1.8326	102.68
LB-0.55	463.16	0.2116	1.8278	106.41
LB-0.68	532.21	0.2412	1.813	122.28
LB-0.7	540.18	0.2496	1.809	126.11

According to the adsorption-desorption isotherm of carbon molecular sieve (Fig. 2), it conforms to the type I adsorption isotherm, namely the Langmuir isotherm equation. This indicates that the prepared carbon molecular sieve's microporous structure is relatively developed [24].

The pore size distribution of carbon zeolite also confirmed this structure. As shown in Fig. 3, the pore size distribution of the two samples has obvious peak values between 0–1 nm and small peak values between 1–2 nm, indicating that both samples have a relatively developed micropore structure, which also reflects that boric acid has a good activation effect and is primarily made up of micropores.

The boric acid activated *Stellera Chamaejasme*-based carbon molecular sieve has two peaks, and its pore-making trend is micropore and ultra-pore, as shown in the figure. Phosphoric acid, on the other hand, is mesoporous and has similar physical and chemical properties to boric acid. The average pore size of the higher peak in LB-0.55 was 0.683 nm, while the lower peak's average pore size was 1.399

nm. The lower peak gradually approached the higher peak as impregnation increased, and the average pore size changed from 1.399 to 0.973 nm, but the higher peak's original average pore size did not change much. The results show that as the amount of boric acid impregnation increases, the pore size of the micropores becomes more similar to that of the micropores.
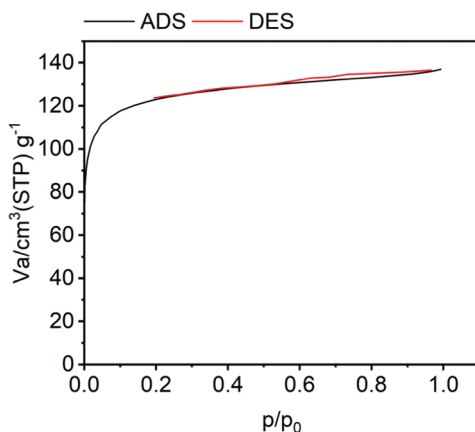

Figure 2: Adsorption-desorption isotherms
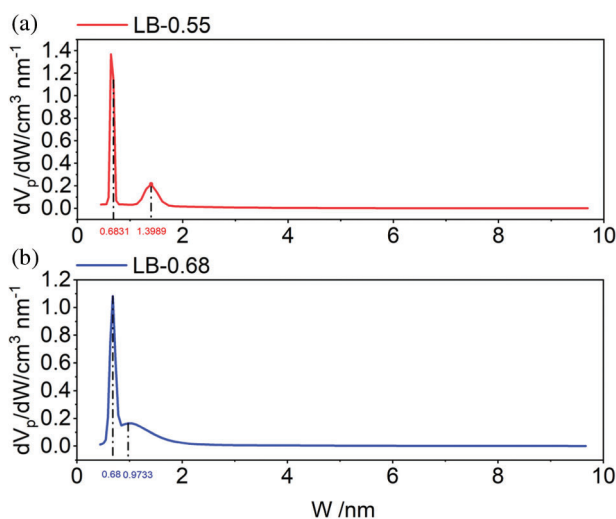
Figure 3: (a) The aperture distribution of LB-0.55 (b) The aperture distribution of LB-0.68

As can be seen in Fig. 4, as the loading capacity increases, the surface smooths out and the morphology becomes more regular. This is due to the fact that the observation phenomenon has shifted from larger to smaller pore sizes. This also backs up the pore size distribution characterization conclusion. The specific surface area of the prepared carbon molecular sieve is increased due to the presence of a large number of micropores, resulting in improved adsorption performance.

We also did elemental analysis on the samples at the same time. The majority of the sample is made up of carbon, with only about 3% of the sample containing boron (LB-0.68). The amount of B doping in LB-0.55 was only 1.2 percent, implying that the formation of ultrafine pores is related to the amount of B doping.
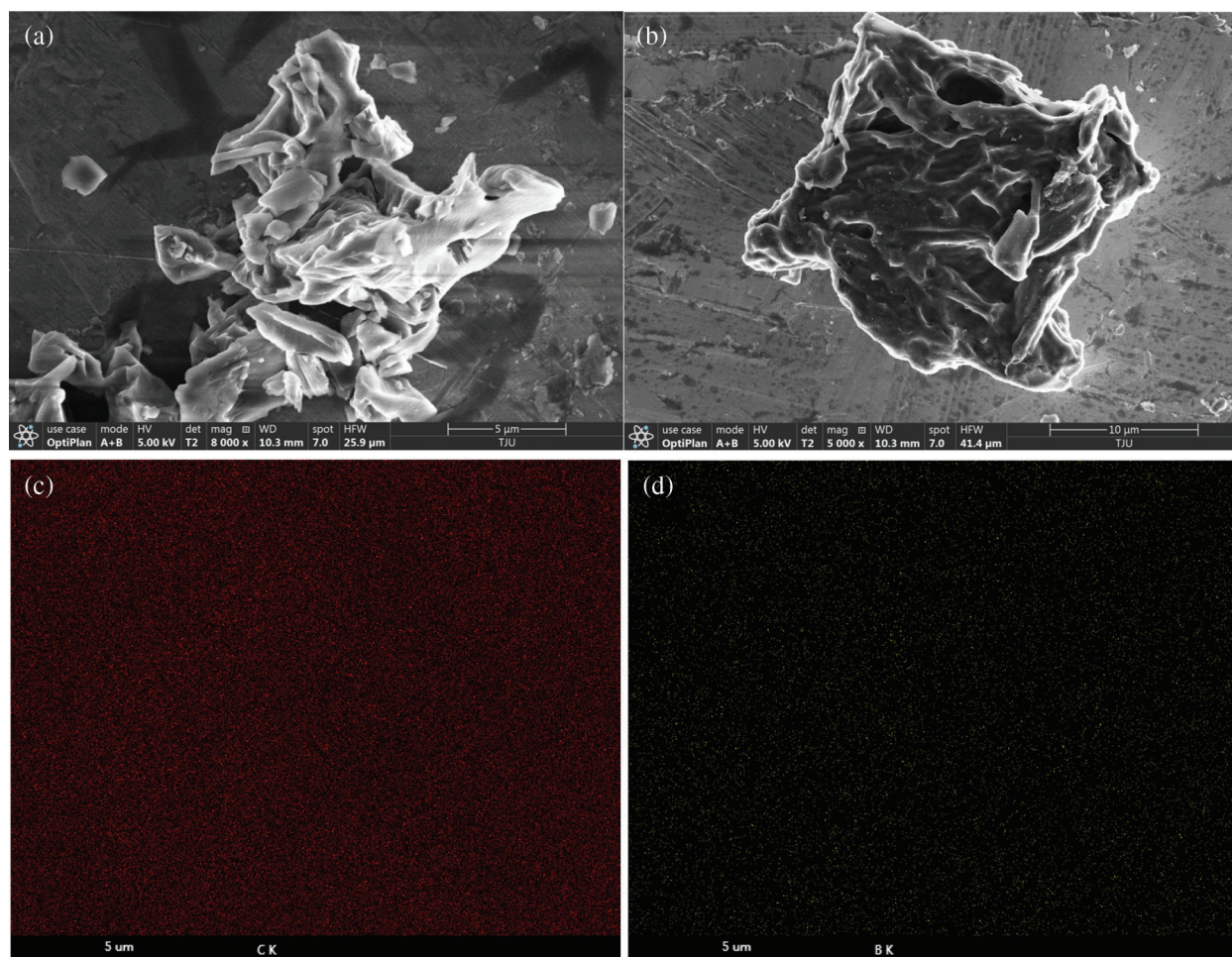
Figure 4: (a) SEM of inactivated samples (b) SEM of activated samples (c) & (d) Elemental analysis of LB-0.68

The surface of the sample had numerous and uniform micropores, according to TEM (Fig. 5) analysis. The fact that the samples are carbon molecular sieves is further supported by their regular shape and dense distribution.

The carbon structure is very sensitive to the Raman spectra (Fig. 6), which has a significant peak effect in the wave number range of 0–3300 cm^{-1}. The corresponding frequency range of Raman spectra for graphite-like materials is 0–3300 cm^{-1}, with 0–1650 cm^{-1} being the First-order region and 1650–3300 cm^{-1} being the Second-order region [25]. Wave numbers corresponding to Raman spectrum lines are divided into three categories. The natural G-line of natural graphite is the first. Within the ideal graphite lattice plane, the stretching vibration mode of C-C is E_{2g2}. The D-line, which is caused by disordered structure and is located near 1360 cm^{-1}, belongs to the A_{1g} vibration mode of the graphite base plane. The spectral line does not exist in single crystal graphite, but it increases as the disordered structure and microcrystalline size decrease. Finally, there are other spectral lines in the disordered structure of carbon materials near 1180, 1500, 1620 cm^{-1}, expect the G and D lines. Some researchers believed that the amorphous carbon or some functional groups in the sample were the reasons for these spectral lines [26].
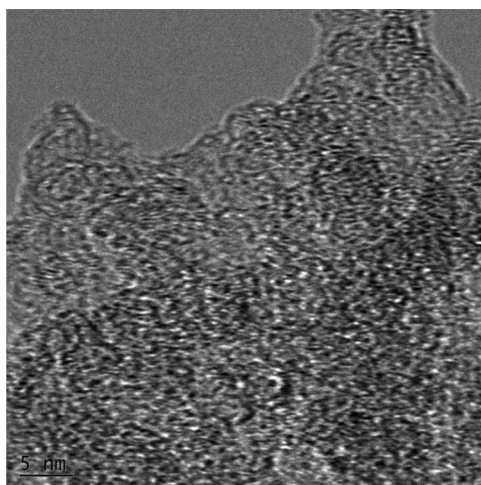
Figure 5: TEM analysis
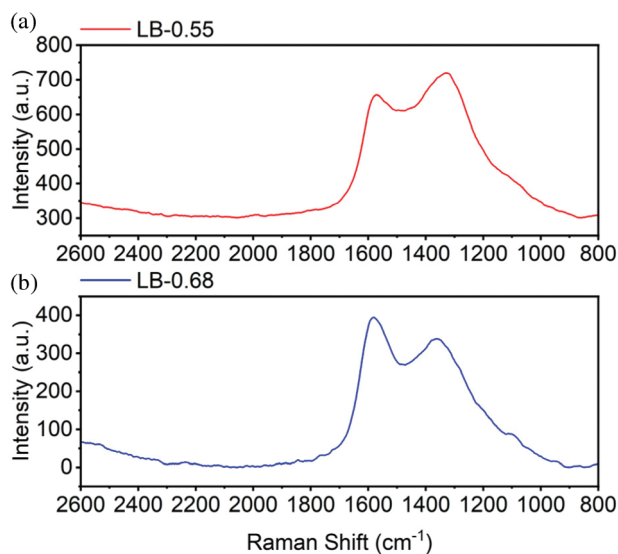
**Figure 6:** (a) Raman of LB-0.55 (b) Raman of LB-0.68

The ratio R of integral intensity between D peak of disordered structure and G peak of ordered structure, namely, the following equation, is used to define graphitization of carbon materials in Raman spectrum:

$$R = \frac{A_D}{A_G}$$

Fitting the respective peaks of related spectrum peaks yielded the integral areas AD of peak D and AG of peak G. The Raman spectra of LB-0.55 and LB-0.68 are shown in Fig. 8. Both samples show typical saddle-shaped Raman spectrum peaks of graphite carbon, indicating that graphitization occurs in both samples during activation, as shown in the figure. The R of LB-0.55 was 1.2, and there was no other disordered structure peak in the first-order region, indicating that the sample was highly graphitized, had a relatively orderly structure, and was chemically stable. The R of LB-0.68 was 0.8, and there was no other disordered structure peak in

the first-order region, indicating that the graphitization degree of the sample would increase as the amount of boric acid impregnation increased, and it would have better chemical stability.

In the XRD pattern shown in Fig. 7, the signature peak of amorphous carbon, also known as the "Steamed Bun Peak," decreases in intensity as impregnation increases. This could be due to the carbon material's increasing crystallinity.
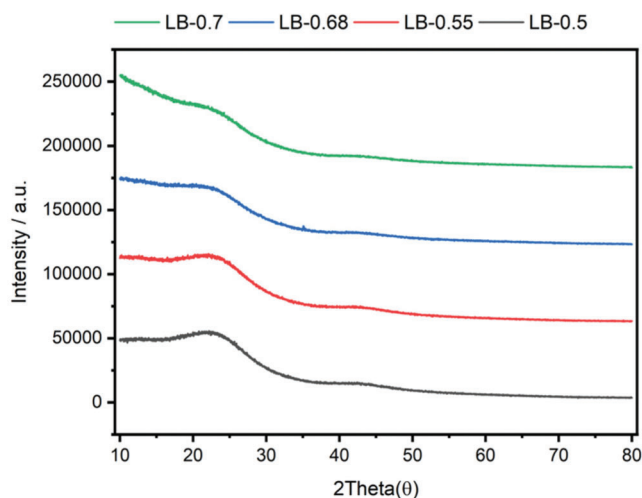
Figure 7: XRD of different samples
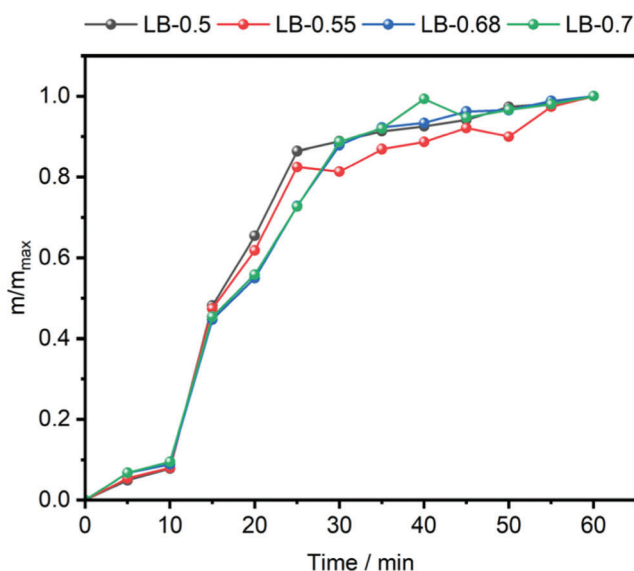
Figure 8: Adsorption kinetics of LB

The XRD figure of samples with different impregnation amounts shows that as the amount of impregnation increases, the degree of amorphous carbon decreases. This is also supported by the Raman spectra of characterization results, which show that improved dipping can lead to the same amount of activation temperature, higher graphitization degree, and better chemical stability.

Adsorption kinetics should be fast for a good adsorbent. methylene blue adsorption kinetics on LB at 25°C were investigated. The saturated adsorption capacity reaches 90% in about 25 min, as shown in Fig. 8 (The m denotes the current adsorption capacity and the m_{max} denotes the adsorption capacity at adsorption equilibrium), indicating that the methylene blue adsorption speed is very fast. In terms of practical application, the *Stellera-Chamaejasme*-Based molecular sieve's fast kinetic rate can reduce adsorption time and increase work efficiency.

When compared to other carbon molecular sieves' adsorption kinetics [27], LB's adsorption kinetics are consistent, proving that the prepared materials are carbon molecular sieves. Its adsorption performance is also improved due to the large number of ultra-porous structures.

4 Conclusions

(1) Boric acid impregnation can be used to make bio-based carbon molecular sieve from Qinghai Province's characteristic biomass roots. The results show that sample LB-0.68 has the best activation effect when the impregnation concentration is 30%, and that the activation effect does not improve significantly as the concentration is increased.

(2) The prepared *Stellera-Chamaejasme*-Based carbon molecular sieve had a relatively developed microporous structure, according to BET characterization. The pore size distribution has two obvious peaks at 0–1 nm and 1–2 nm, and as the impregnation amount increases, the peak of average pore size of 1.399 nm gets closer to the peak of average pore size of 0.683 nm. This demonstrates that the boric acid impregnation method is primarily used to create micropores, with the pore-making trend tending toward superfine pores as the impregnation concentration is increased.

(3) The results of the prepared *Stellera-Chamaejasme*-Based carbon molecular sieve's Raman spectrum and XRD characterization show that the samples have a high degree of graphitization, and that as the impregnation amount is increased, the graphitization degree will significantly increase at the same activation temperature.

(4) The characterization results of BET pore size distribution were verified through the determination of adsorption values, and it was determined that there are two relatively concentrated pore size distribution peaks of *Stellera-Chamaejasme*-Based carbon molecular sieve, and it has a good adsorption effect on iodine.

As a result, this paper investigated the activation effect of boric acid on *Stellera Chamaejasme*, and boric acid was found to be an excellent activator. The determination of iodine adsorption value, which tended to be smaller than 1 nm ultra-fine pores, confirmed the concentration of pore formation tendency.

Availability of Data and Materials: All experimental data can be obtained by contacting the corresponding author.

Conflicts of Interest: The authors declare that they have no conflicts of interest to report regarding the present study.

Reference

1. Wu, Z. X., Webley, P. A., Zhao, D. Y. (2012). Post-enrichment of nitrogen in soft-templated ordered mesoporous carbon materials for highly efficient phenol removal and CO_2 capture. *Journal of Materials Chemistry, 22(22),* 11379–11389. DOI 10.1039/c2jm16183d.

2. Xing, A. H., Li, Y., Xue, Y. P., Jiang, L. X., Zhu, W. P. et al. (2010). Progress in application of SAPO-34 molecular sieves. *Industrial Catalysis, 18(11),* 10–18. DOI 10.3969/j.issn.1008-1143.2010.11.002.

3. Zhou, L. L., Yu, L., Zhao, Y. M., Zhang, X., Chen, Z. P. (1992). Study on the application technology of carbon molecular sieve air conditioner in garlic storage. *Journal of Beijing Agricultural University, 1992(1),* 47–51.

4. Song, G. D., Jiang, Z. W. (1987). Application of carbon molecular sieve in gas chromatographic analysis. *Chromatographic, 1987(1),* 58–59.

5. Liu, Q. Y., Fan, W. (2021). New progress in preparation of mesoporous molecular sieves-secondary synthesis, supramolecular self-assembly and mesoporous generating agent method. *Chinese Journal of Chemistry, 42(1),* 60–73. DOI 10.1002/cjoc.19970150112.

6. Ma, A. L., Huang, G. X., Geng, Q. H., Yao, Y. H., Li, Y. Y. et al. (2021). Preparation and electrochemical properties of Boron/Nitrogen co-doped porous carbon nanosheets. DOI 10.16085/j.issn.1000-6613.2019-1991.

7. Wu, X. T. (2020). *Preparation of heteroatom doped biomass porous carbon and its application in supercapacitors (Master Thesis).* University of North, China.

8. Zeng, X. X. (2020). *Synthesis, structure and electrochemical properties of a new transition metal borate (Master Thesis).* South China University of Technology, China.

9. Jiang, P. (2020). *Design and properties of non-noble Metal Carbon based oxygen reduction/precipitation catalyst (Master Thesis).* Beijing University of Chemical Technology, China.

10. Zhai, Y. Y. (2020). *Application of biomass-derived carbon materials in heterogeneous catalytic reaction and energy storage (Master Thesis).* Hebei University, China.

11. Suo, N. (2020). *Preparation and catalytic performance of boron doped carbon materials for oxygen reduction (Master Thesis).* Dalian University of Technology, China.

12. Wang, G. X., Cheng, G. D. (2001). Characteristics and ecological changes of grassland resources in river headwaters region. *China Desert, 2001(2),* 101–107. DOI 10.3321/j.issn:1000-694X.2001.02.001.

13. Song, M. L., Wang, Y. Q., Bao, G. S., Wang, H. S. (2020). Effects of *Stellera Chamaejasme* control on plant nutrient reuptake in alpine grassland communities. *Journal of Grass Industry, 29(10),* 47–57. DOI 10.11686/cyxb2019548.

14. You, Y. F., Ma, Q. C., Guo, Y. Z., Kong, Y. Z., Shi, F. Y. et al. (2018). The harm status and control countermeasures of poisonous grass in natural grassland of inner mongolia. *Advances in Veterinary Medicine, 39(4),* 105–110. DOI DOI 10.3969/j.issn.1007-5038.2018.04.022.

15. Liu, Y., Ling, R. J., Yao, T. (2004). Advances in studies of *Stellera Chamaejasme* in grassland. *Pratacultural Science, 2004(6),* 55–61. DOI 10.3969/j.issn.1001-0629.2004.06.017.

16. Cui, X., Pan, Y., Wang, Y. N., Zheng, X. N., Gao, Y. (2020). Effects of *Stellera Chamaejasme* on small-scale community composition and soil physicochemical properties in degraded grassland. *Chinese Journal of Ecology, 39(8),* 2581–2592. DOI 10.13292/j.1000-4890.202008.017.

17. Huang, Z. J., Zhou, S. Q. (1993). Important poisonous plant of grassland–*Stellera Chamaejasme*. *Sichuan Grassland, 1993(4),* 24–27.

18. Feng, W. X., Lu, X., Xu, K. T., Yu, Z. X., Tang, C. et al. (2019). Research progress on medicinal components and allelopathy of *Stellera Chamaejasme* in natural grassland. *Advances in Veterinary Medicine, 40(12),* 84–88. DOI 10.16437/j.cnki.1007-5038.2019.12.017.

19. Li, H. C., Huang, L. J., Sun, H. Z. (2019). Study on the preparation of furfural by stele and the characteristics of raw materials of stele. *China Agricultural Science and Technology Herald, 21(9),* 137–142. DOI 10.13304/j.nykjdb.2018.0510.

20. Zhang, N., He, J., Ding, K., Zhang, Y. Y., Ma, B. Z. et al. (2020). Study on chemical constituents of *Stellera Chamaejasme*. *Chinese Journal of Pharmacy, 55(10),* 799–805. DOI 10.11669/cpj.2020.10.009.

21. Chen, J. (2015). *Study on preparation and adsorption properties of Stellera Chamaejasme activated carbon (Master Thesis)*. Tianjin University, China.

22. He, Y. N., Wang, X. M., Wang, J. W. (2021). Preparation and adsorption properties of activated carbon hydrogel from xanthocorpa. *Applied Chemical Industry, 50(6),* 1563–1568. DOI 10.16581/j.cnki.issn1671-3206.20210326.001.

23. Yi, X. W., Yang, H. M., Turson, T. (2021). Preparation and characterization of biochar based on padan wood shell. *Journal of Materials Science and Engineering, 39(2),* 322–329. DOI 10.14136/j.cnki.issn1673-2812.2021.02.026.

24. Behere, K., Yoon, S. (2021). N-layer BET adsorption isotherm modeling for multimeric protein A ligand and its lifetime determination. *Journal of Chromatography B,* 1162, 122434.

25. He, J. J., Lv, C. X., Li, D. H. (2020). Microstructure characterization of carbon fibers by Raman spectroscopy. *Chemical Progress, 39(S2),* 227–233. DOI 10.16085/j.issn.1000-6613.2020-0507.

26. Carotenuto, G., Longo, A., Camerlingo, C., Nicola, S. D., Pepe, G. P. (2016). Polarity microraman spectroscopy of carbon nanocoils. *New Carbon Material, 31(6),* 621–627. DOI 10.1016/S1872-5805(16)60036-7.

27. Zeinab, E., Batonneau-Gener, I., Pouilloux, Y., Hamad, H. (2016). Removal of methylene blue by mesoporous CMK-3: Kinetics, isotherms and thermodynamics. *Journal of Molecular Liquids, 223,* 763–770. DOI 10.1016/j.molliq.2016.09.003.